

# Gross-Pitaevskii Equation and Center of Mass Motion in Spin-Orbit Coupled Bose-Einstein Condensates

Yongping Zhang, Li Mao, and Chuanwei Zhang\*

*Department of Physics and Astronomy, Washington State University, Pullman, WA, 99164 USA*

We derive the mean-field Gross-Pitaevskii equation for spin-orbit coupled Bose-Einstein condensates by taking account that the pseudospin states of atoms are superpositions of the hyperfine states with different scattering lengths. The ground state phases of the condensate in a harmonic trap are obtained numerically in various parameter regions. We find a new oscillation period in the center of mass motion of the condensate subject to a sudden shift of the harmonic trap. The oscillation period is dependent on the direction of the shift of the harmonic trap, linearly proportional to the spin-orbit coupling strength, and independent on the interaction strength.

PACS numbers: 03.75.Mn, 03.75.Kk, 71.70.Ej, 37.10.Vz

Spin-orbit coupling (SOC) for electrons plays a crucial role in many important phenomena and applications in the solid state, such as anomalous and spin Hall effects [1], topological insulator [2], spintronic devices [3], *etc.* Motivated by emulating condensed matter phenomena with cold atoms and developing atomtronic devices [4], the study of SOC for ultra-cold neutral atoms has drawn a lot of interest recently [5–21]. A significant difference between electrons and atoms is that, while electrons are fermions, ultra-cold atoms may be bosons, leading to novel spin-orbit physics that has not been fully explored in the solid state. Remarkably, substantial experimental progress toward implementing SOC in a Bose-Einstein condensate (BEC) has been made recently [16].

The starting point for studying the dynamics of a BEC is the Gross-Pitaevskii (G-P) equation, which describes the many-body atom interaction within the mean-field approximation [22]. In a regular spinor BEC, where the pseudospins are defined as the atom hyperfine states, the mean-field interaction strength between two spin components is determined by their *s*-wave scattering length, and the corresponding interaction energy depends on the atom density. Recently, this mean-field description has been extended to spin-orbit coupled BECs by assuming the scattering interaction between atoms depends only on their pseudospin states [19–21]. However, such a simple treatment may not work in general because the pseudospin states in many schemes for implementing SOC are the superpositions of the hyperfine states with different scattering lengths.

In this Letter, we derive a generic G-P equation for spin-orbit coupled BECs, where the mean-field interaction terms in the pseudospin space are obtained by taking account of different *s*-wave scattering lengths for different hyperfine components of pseudospin states. Because different laser configurations for the implementation of SOC yield different superpositions of hyperfine states for a pseudospin state, the corresponding G-P equations are also different. In general, the mean-field interaction energy may depend not only on the density, but also the

phase of the condensate (*i.e.*, terms like  $\Psi_1^2 \Psi_2^{*2} + c.c.$ ), which, to the best of our knowledge, have not been explored before. This G-P equation may serve as the starting point for studying the dynamics of spin-orbit coupled BECs.

As examples, we consider two laser setups for realizing the Rashba SOC. The G-P equation in one setup (denoted as the simple system) is the same as that for a regular spinor condensate, while new terms containing the condensate phases emerge in the G-P equation for the other setup (denoted as the complex system). We analyze the condensate wavefunctions for both simple and complex systems in various parameter regions. In the strong interaction and SOC region, there exist two distinct phases for the condensate density: Thomas-Fermi (TF) and stripe. While in the weak and medium interaction or SOC region, spatial separation between two pseudospin components is observed. The low energy collective excitations in spin-orbit coupled BECs are investigated through the center-of-mass (COM) motion of the condensate when a sudden shift of the harmonic trap is applied. In the TF phase of the simple system, a new oscillation frequency in the COM motion, in addition to the harmonic trap frequency, develops when the shift of the harmonic trap is perpendicular to the direction of the condensate phase variation, but does not exist when they are parallel. The oscillation period is linearly proportional to the SOC strength, but independent on the atom interaction strength, although the oscillation amplitude decays in the weak interaction region. In the complex system, both oscillation period and amplitude are strongly modified from that in the simple system, even though they share the same physical parameters.

Consider ultra-cold bosonic atoms confined in a quasi-two-dimensional (*xy* plane) harmonic trap with a tripod electronic level scheme (Fig. 1a). The atom dynamics along the  $\hat{z}$  direction are frozen by a deep optical trap or lattice. The hyperfine ground states  $|1\rangle$ ,  $|2\rangle$ ,  $|3\rangle$  are coupled with the excited state  $|0\rangle$  using three blue-detuned lasers with the Rabi frequencies  $\Omega_1$ ,  $\Omega_2$ , and

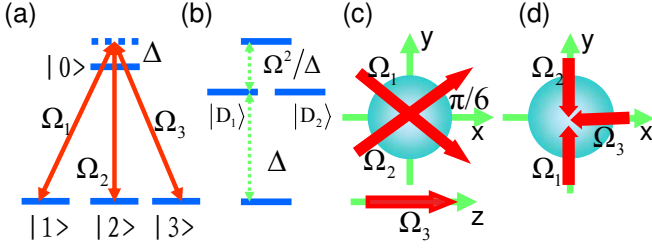


Figure 1. (Color online) A tripod scheme for implementing Rashba spin-orbit coupling. (a) The atom-laser coupling. (b) Energy levels.  $|D_1\rangle$  and  $|D_2\rangle$  are degenerate dark states.  $\Omega = \sqrt{|\Omega_1|^2 + |\Omega_2|^2 + |\Omega_3|^2}$ . (c,d) Two different laser configurations [9, 17].

$\Omega_3$ . The Hamiltonian of the system can be written as  $H = \sum_i H_s(\mathbf{r}_i) + H_{int}$  with the single particle Hamiltonian

$$H_s(\mathbf{r}) = \mathbf{p}^2/2m + V(\mathbf{r}) + H_I(\mathbf{r}), \quad (1)$$

where  $V(\mathbf{r}) = m(\omega_\perp^2 r^2 + \omega_z^2 z^2)/2$  is the harmonic trapping potential with the corresponding trapping frequencies  $\omega_z$  and  $\omega_\perp$ .  $H_I(\mathbf{r}) = -\hbar\Delta|0\rangle\langle 0| - \hbar(\Omega_1|0\rangle\langle 1| + \Omega_2|0\rangle\langle 2| + \Omega_3|0\rangle\langle 3| + H.c.)$  describes the atom-laser interaction, and  $\Delta$  is the detuning to the state  $|0\rangle$ . The diagonalization of the Hamiltonian  $H_I(\mathbf{r})$  yields two degenerate dark states  $|D_1\rangle = \sum_{\alpha=1}^3 d_\alpha(\mathbf{r})|\alpha\rangle$ ,  $|D_2\rangle = \sum_{\alpha=1}^3 f_\alpha(\mathbf{r})|\alpha\rangle$  and two bright states (Fig. 1b), where the coefficients  $d_\alpha(\mathbf{r})$ ,  $f_\alpha(\mathbf{r})$  are determined by the parameters  $\Omega_i$  and  $\Delta$ . In experiments, a large detuning  $\Delta$  is chosen to suppress the spontaneous emission of photons that heats the atom gas. The blue-detuned lasers are used to ensure the degenerate dark states are the ground states of the system to avoid the loss from three-body collisions. In the subspace spanned by the pseudospin states  $|\uparrow\rangle \equiv |D_1\rangle$  and  $|\downarrow\rangle \equiv |D_2\rangle$ ,

$$H_s(\mathbf{r}) = \mathbf{p}^2/2m + \gamma(p_x\sigma_y - p_y\sigma_x) + V(\mathbf{r}), \quad (2)$$

where  $\gamma$  is the Rashba SOC strength. The  $s$ -wave scattering interaction between atoms can be written as  $H_{int} = \sum_{i<j} \sum_{\alpha,\beta=1}^3 g_{\alpha\beta} \delta(\mathbf{r}_i^\alpha - \mathbf{r}_j^\beta)$ , where  $\mathbf{r}_i^\alpha$  is the position of the atom  $i$  in the hyperfine state  $\alpha$ ,  $g_{\alpha\beta} = 4\pi\hbar^2 a_{\alpha\beta}/m$ ,  $a_{\alpha\beta}$  is the  $s$ -wave scattering length between atoms in the hyperfine states  $|\alpha\rangle$  and  $|\beta\rangle$ .

In the Hartree approximation, the many-body wavefunction of the bosonic system can be taken as the product of the single-particle wave function  $|\Psi(\mathbf{r}_1, \mathbf{r}_2, \dots, \mathbf{r}_N)\rangle = \prod_{i=1}^N |\Phi(\mathbf{r}_i)\rangle$ , where  $|\Phi(\mathbf{r})\rangle = \Phi_\uparrow(\mathbf{r})|D_1(\mathbf{r})\rangle + \Phi_\downarrow(\mathbf{r})|D_2(\mathbf{r})\rangle$  with the normalization condition  $\int d\mathbf{r} (|\Phi_\uparrow(\mathbf{r})|^2 + |\Phi_\downarrow(\mathbf{r})|^2) = 1$ . The G-P equation can be obtained through the minimization of the mean-field energy functional  $E(\Phi_\uparrow, \Phi_\downarrow) = \langle \Psi | H | \Psi \rangle$  with respect to  $\Phi_\uparrow$  and  $\Phi_\downarrow$  [22]. Because the scattering length is between atoms in different hyperfine states, the interaction energy  $\langle \Psi | H_{int} | \Psi \rangle$  should be evaluated within the

hyperfine state basis, *i.e.*,  $|\Phi(\mathbf{r})\rangle = \sum_{\alpha=1}^3 [\Phi_\uparrow(\mathbf{r})d_\alpha(\mathbf{r}) + \Phi_\downarrow(\mathbf{r})f_\alpha(\mathbf{r})]|\alpha\rangle$ , from which we derive the G-P equation for a spin-orbit coupled BEC

$$i\hbar\partial\Phi/\partial t = H_s\Phi + \Gamma\Phi. \quad (3)$$

Here the two component wavefunction  $\Phi = (\Phi_\uparrow, \Phi_\downarrow)^T$  in the pseudospin basis  $\{|\uparrow\rangle, |\downarrow\rangle\}$ . The nonlinear term  $\Gamma = \begin{pmatrix} \Gamma_1 & \Gamma_2 \\ \Gamma_2^* & \Gamma_3 \end{pmatrix}$ , where  $\Gamma_1 = C_1|\Phi_\uparrow|^2 + C_2|\Phi_\downarrow|^2 + 2\text{Re}(C_3\Phi_\uparrow^*\Phi_\downarrow)$ ,  $\Gamma_2 = C_3|\Phi_\uparrow|^2 + C_4|\Phi_\downarrow|^2 + C_5\Phi_\uparrow^*\Phi_\downarrow$ , and  $\Gamma_3 = C_2|\Phi_\uparrow|^2 + C_6|\Phi_\downarrow|^2 + 2\text{Re}(C_4\Phi_\uparrow^*\Phi_\downarrow)$ . The nonlinear coefficients  $C_1 = 2N\sum_{\alpha,\beta=1}^3 g_{\alpha\beta}|d_\alpha|^2|d_\beta|^2$ ,  $C_2 = 2N\sum_{\alpha,\beta=1}^3 g_{\alpha\beta}(|d_\alpha|^2|f_\beta|^2 + d_\alpha^*f_\alpha d_\beta f_\beta^*)$ ,  $C_3 = 2N\sum_{\alpha,\beta=1}^3 g_{\alpha\beta}|d_\alpha|^2 d_\beta^* f_\beta$ ,  $C_4 = 2N\sum_{\alpha,\beta=1}^3 g_{\alpha\beta}|f_\alpha|^2 d_\beta^* f_\beta$ ,  $C_5 = 2N\sum_{\alpha,\beta=1}^3 g_{\alpha\beta}d_\alpha^* f_\alpha d_\beta^* f_\beta$ , and  $C_6 = 2N\sum_{\alpha,\beta=1}^3 g_{\alpha\beta}|f_\alpha|^2|f_\beta|^2$ .  $C_3$ ,  $C_4$  and  $C_5$  terms, which are absent in previous study, originate from the linear superposition of hyperfine states for a pseudospin state. We see that not only the density, but also the relative phase between two components, play an important role on the dynamics of the BEC.

For simplicity, we assume  $g_{\alpha\beta} = g_1$  for  $\alpha \neq \beta$  and  $g_{\alpha\beta} = g_0$  for  $\alpha = \beta$  with the corresponding scattering lengths  $a_1$  and  $a_0$ , although the nonlinear G-P equation (3) works for any  $g_{\alpha\beta}$ .  $C_3$ ,  $C_4$ ,  $C_5 \propto g_0 - g_1$  and vanish when  $g_0 = g_1$ . In this case, the nonlinear term  $\Gamma$  is the same as that for a regular spinor BEC.  $C_i$  depend strongly on the laser configurations for implementing the Rashba SOC. Here we consider two setups (Figs. 1c and 1d) that have been investigated previously in the literature [9, 17]. In the first setup (Fig. 1c), we have  $C_3 = C_4 = C_5 = 0$ ,  $C_1 = C_6 = 4N\sqrt{2\pi m\omega_z/\hbar}(a_0 + 2a_1)/3$ , and  $C_2 = 4N\sqrt{2\pi m\omega_z/\hbar}(2a_0 + a_1)/3$  (the simple system). Here we rescale the G-P equation (3) with the time and length units  $\omega_\perp^{-1}$  and  $\sqrt{\hbar/m\omega_\perp}$  respectively. In the second setup (Fig. 1d), all of  $C_i$  are nonzero, and the nonlinear term  $\Gamma$  has a complex form (the complex system).

We numerically solve the G-P equation (3) using the imaginary time evolution method and obtain the ground state of the condensate. In the simple system, there are two different types of phases in the region of strong SOC ( $\gamma \gg 1$ ) and interaction ( $C_i \gg 1$ ): the Thomas-Fermi (TF) phase when  $C_1 \geq C_2$  (Fig. 2a) and the stripe phase when  $C_1 < C_2$  (Fig. 2c) [19]. In the TF phase, the maximum densities of two components locate at the harmonic trap center, but the phase of the condensate varies like a plane wave  $\exp(i\mathbf{k} \cdot \mathbf{r})$  (Fig. 2b). In the stripe phase, the density for each pseudospin component forms a set of stripes (Fig. 2c) and two components are spatially separated. There is a sharp change of the condensate phase in and outside the stripe region (Fig. 2d). The total density of two components has a TF distribution for both phases. The direction of the condensate phase vari-

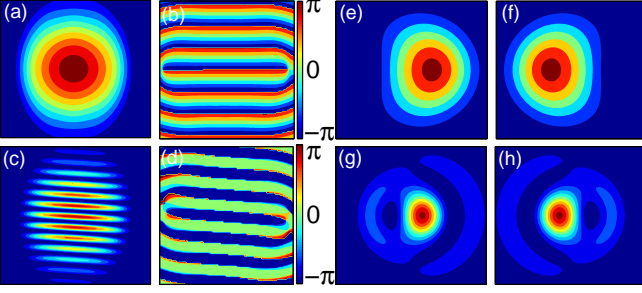


Figure 2. (Color online) Condensate wavefunction  $\Phi$  in the simple system. (a,b) Density  $|\Phi_\uparrow|^2$  (a) and phase  $\arg(\Phi_\uparrow)$  (b) in the TF phase.  $C_1 = 10$ ,  $C_2 = 6$ ,  $\gamma = 10$ . (c,d) In the stripe phase.  $C_1 = 6$ ,  $C_2 = 10$ ,  $\gamma = 10$ . (e,f) Density  $|\Phi_\uparrow|^2$  and  $|\Phi_\downarrow|^2$  with  $C_1 = 10$ ,  $C_2 = 6$ ,  $\gamma = 1$ . (g,h) Density  $|\Phi_\uparrow|^2$  and  $|\Phi_\downarrow|^2$  with  $C_1 = C_2 = 0$ ,  $\gamma = 10$ .

ation  $\nabla \arg(\Phi_\sigma)$  is spontaneously selected, along which the density distribution is wider. We find that the density profile in each hyperfine state has the same structure (TF or stripe) as that in the pseudospin state, therefore the TF and stripe phases should be observable by directly measuring the density in each hyperfine state.

In the medium SOC region ( $\gamma \sim 1$ ), there exists spatial separation between the atom densities of two pseudospin components when  $C_1 \geq C_2$  (Figs. 2e, 2f). The separation can be understood from the spin-dependent force  $\mathbf{F} = \frac{d\mathbf{p}}{dt} = 2\gamma^2(\mathbf{k} \times \hat{e}_z)\sigma_z$  generated by the Rashba SOC, where  $\mathbf{k}$  is the momentum of atoms and along the condensate phase variation direction.  $\mathbf{F}$  has the opposite directions for two pseudospins and is along the  $\hat{\mathbf{x}}$  direction when the phase variation is along the  $\hat{\mathbf{y}}$  direction (Fig. 2b), leading to the spatial separation of two pseudospin components along the  $\hat{\mathbf{x}}$  direction (Figs. 2e, 2f). The separation due to the spin-dependent force is more transparent in the non-interacting region (Figs. 2g, 2h) without involving the complexity from the interaction. However, the separation between two components decreases not only for very strong SOC ( $\gamma \gg 1$ , Fig. 2a), but also for very weak SOC ( $\gamma \ll 1$ ), which can be understood based on  $\mathbf{F} \propto \gamma^2$  and the zero separation for a regular spinor BEC without SOC.

In the complex system, similar TF and stripe phases also exist in the strong SOC and interaction region. However, significant differences between the simple and complex systems exist for the low energy collective excitations even though their condensate phases are similar. Here we consider the COM motion of the condensate subject to a sudden shift of the harmonic trap. It is well-known that the COM motion of a BEC without SOC is a dipole oscillation whose frequency is the harmonic trap frequency and does not depend on the nonlinearity [23]. On the other hand, the interference between two Rashba spin-orbit energy bands yields the Zitterbewegung (ZB) oscillation [10] for a single particle in the free space with

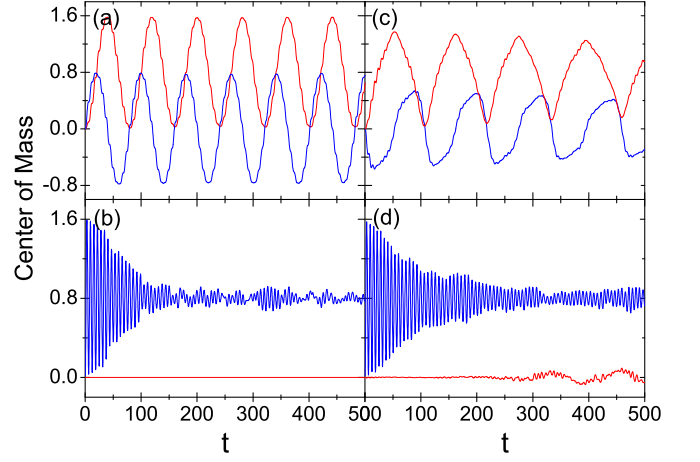


Figure 3. (Color online) The center of mass motion. Red lines:  $\langle x \rangle$ ; Blue lines:  $\langle y \rangle$ . (a,b) The simple system with the corresponding condensate wavefunction in Figs. 2a and 2b. The shift of the harmonic trap  $D = 0.8$ . The shifts are along the  $\hat{\mathbf{x}}$  (a) and  $\hat{\mathbf{y}}$  (b) directions respectively. (c,d) The same COM motion as (a,b) but for the complex system. Parameters are the same as that in (a,b) except that new terms  $C_3$ ,  $C_4$ ,  $C_5$  are included in the condensate and COM motion calculations.

the oscillation period inversely proportional to  $\gamma^2$ . In this Letter, we study the COM motion of a BEC in the presence of interaction, a harmonic trap, and Rashba SOC.

The COM motion

$$\langle \mathbf{r}(t) \rangle = \int (|\Phi_\uparrow(\mathbf{r}, t)|^2 + |\Phi_\downarrow(\mathbf{r}, t)|^2) \mathbf{r} d\mathbf{r} \quad (4)$$

of the condensate can be obtained by numerically solving the G-P equation (3) and is plotted in Figs. 3a and 3b (Figs. 3c, 3d) for the TF phase in the simple (complex) system. In the simple system, when the shift of the harmonic trap is along the  $\hat{\mathbf{x}}$  direction (perpendicular to the condensate phase variation  $\nabla \arg(\Phi_\uparrow)$  direction  $\hat{\mathbf{y}}$ ), the COM motion along the  $\hat{\mathbf{x}}$  direction is perfectly periodic with two periods (Fig. 3a): one corresponds to the harmonic trap frequency, the other is much larger and linearly proportional to the SOC strength  $\gamma$  (Fig. 4). The COM motion along the  $\hat{\mathbf{y}}$  direction is similar. However, when the shift of the harmonic trap is along the  $\hat{\mathbf{y}}$  direction, the COM motion along the  $\hat{\mathbf{y}}$  direction possesses only the harmonic trap frequency and the oscillation amplitude is strongly damped (Fig. 3b). The COM motion along the  $\hat{\mathbf{x}}$  direction vanishes.

The different COM motions along different shifting directions may be understood from the single atom dynamics with the Rashba SOC. The spin-orbit coupled atoms have two bands with energies  $E_\pm = \hbar^2 k^2 / 2m \pm \gamma k$  and corresponding wavefunctions  $\phi_\pm = \exp(i\mathbf{k} \cdot \mathbf{r})(1, \pm i e^{i\varphi_{\mathbf{k}}})^T / \sqrt{2}$ , where  $\varphi_{\mathbf{k}} = \arg(k_x + ik_y)$ . The ground state of the atom  $\phi_-$  stays at the potential minimum located at  $k_0 = \gamma m / \hbar^2$  with the direction of  $\mathbf{k}_0$  spontaneously selected. The shift of the harmonic trap

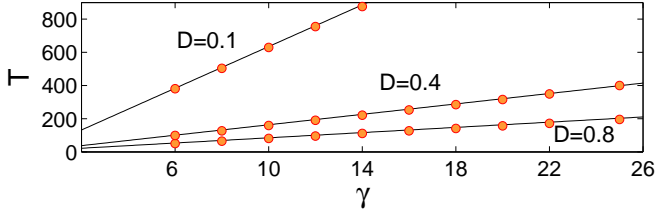


Figure 4. (Color online) Plot of the new COM oscillation period  $T$  with respect to the SOC strength  $\gamma$  for the simple system in the TF phase. Circles are from the numerical stimulation of the G-P equation (3). The lines are from Eq. (5).

corresponds to adding a momentum  $\mathbf{p}$  into the ground state, leading to an initial state  $\phi_{ini} = \exp(i\mathbf{p} \cdot \mathbf{r})\phi_-$ . The time evolution of the wavefunction can be written as  $\varphi(\mathbf{r}, t) = \int d\mathbf{k} [A_- \exp(iE_- t)\phi_- + A_+ \exp(iE_+ t)\phi_+]$ , where  $A_{\pm} = \langle \phi_{\pm} | \phi_{ini} \rangle$ . When  $\mathbf{p}$  is perpendicular to the direction of  $\mathbf{k}_0$  (Fig. 2b), both  $A_{\pm}$  are nonzero, and there is an interference between two spin-orbit coupled bands, leading to the SOC dependent oscillation of the COM motion (Fig. 3a). In contrast, when  $\mathbf{p}$  is along the direction of  $\mathbf{k}_0$ , one of  $A_{\pm}$  must be zero and there is only one oscillation frequency due to the harmonic trap.

We numerically calculate the new oscillation period  $T$  in Fig. 3a for several different sets of interaction parameters, and find that it does not depend on the interaction strengths  $C_1$  and  $C_2$ , indicating essentially single particle physics in this system. In Fig. 4, we plot the dependence of  $T$  with respect to  $\gamma$  for three harmonic trap shifts  $D$ . The numerical data can be well fitted with an analytic formula

$$T = 2\pi(1 + \gamma/D). \quad (5)$$

We see that the period is linearly proportional to  $\gamma$  and  $D^{-1}$ . In the strong SOC region ( $\gamma \gg 1$ ), the strong SOC couples many harmonic oscillator states and tends to reduce the single particle energy splitting, as confirmed by our numerical calculation, resulting in a large oscillation period. Note that this is very different from the ZB oscillation in the weak SOC region [10], where the oscillation period is proportional to  $\gamma^{-2}$  because the energy splitting between two spin-orbit coupled bands in this region is proportional to  $\gamma^2$ , as confirmed in our numerical simulation. Finally, a smaller shift  $D$  leads to less excitations to the high energy states, yielding a larger COM oscillation period. As  $\gamma \rightarrow 0$ ,  $T \rightarrow 2\pi$ , the oscillation period for the harmonic trap frequency, as expected. In the weak and medium interaction or SOC region, our numerical results show that the oscillation amplitude decays with time due to the phase separation of the densities of two pseudospin components (Figs. 2e-2h) that leads to the decoherence in the COM motion.

In the stripe phase of the simple system, the COM motion is always damped because of the decoherence orig-

inating from the spatial separation of two spin components. Similar as the TF phase, the new oscillation period disappears (emerges) when the shift is along (perpendicular to) the condensate phase variation direction.

The COM motion is strongly modified in the complex system. In Fig. 3c and 3d, we plot the COM motion in the TF phase. Clearly, the direction dependence of the new oscillation period is the same as that for the simple system. However, the oscillation period  $T$  is very different from that in the simple system (Fig. 3a) although the complex system has the same parameters ( $C_1$ ,  $C_2$ ,  $\gamma$ ) as the simple one. A damping of the oscillation amplitude is also observed, in contrast to the perfect oscillation in the simple system. Furthermore, when the shift of the harmonic trap is along the condensate phase variation direction, the COM motion perpendicular to the shift direction emerges after a long time (Fig. 3d), in contrast to the zero motion in the simple system (Fig. 3b).

In summary, we derive a generic mean-field G-P equation for spin-orbit coupled BECs. We obtain the condensate phase in various parameter regions and show that a new oscillation period, originating from the SOC, emerges in the COM motion of the condensate subject to a shift of the harmonic trap. We emphasize that the G-P equation may serve as the starting point for the future study on the dynamics of spin-orbit coupled BECs.

We thank Gang Chen for helpful discussion. This work is supported by the ARO (W911NF-09-1-0248) and the DARPA-YFA (N66001-10-1-4025).

\* cwzhang@wsu.edu

- [1] D. Xiao *et al.*, Rev. Mod. Phys. **82**, 1959 (2010).
- [2] M. Z. Hasan, and C. L. Kane, Rev. Mod. Phys. **82**, 3045 (2010).
- [3] I. Žutić *et al.*, Rev. Mod. Phys. **76**, 323 (2004).
- [4] B. T. Seaman *et al.*, Phys. Rev. A **75**, 023615 (2007).
- [5] J. Ruseckas *et al.*, Phys. Rev. Lett. **95**, 010404 (2005).
- [6] S.-L. Zhu *et al.*, Phys. Rev. Lett. **97**, 240401 (2006).
- [7] X.-J. Liu *et al.*, Phys. Rev. Lett. **98**, 026602 (2007).
- [8] T. D. Stanescu *et al.*, Phys. Rev. Lett. **99**, 110403 (2007).
- [9] G. Jūzeliūnas *et al.*, Phys. Rev. A **77**, 011802(R) (2008).
- [10] J. Y. Vaishnav and C. W. Clark, Phys. Rev. Lett. **100**, 153002 (2008).
- [11] T. D. Stanescu *et al.*, Phys. Rev. A **78**, 023616 (2008).
- [12] C. Wu, and I. Mondragon-Shem, arXiv:0809.3532.
- [13] C. Zhang *et al.*, Phys. Rev. Lett. **101**, 160401 (2008).
- [14] X.-J. Liu *et al.*, Phys. Rev. Lett. **102**, 046402 (2009).
- [15] I. B. Spielman, Phys. Rev. A **79**, 063613 (2009).
- [16] Y.-J. Lin *et al.*, Phys. Rev. Lett. **102**, 130401 (2009); Y.-J. Lin *et al.*, Nature **462**, 628 (2009).
- [17] C. Zhang, Phys. Rev. A **82**, 021607(R) (2010).
- [18] T.-L. Ho and S. Zhang, arXiv:1007.0650.
- [19] C. Wang *et al.*, Phys. Rev. Lett. **105**, 160403 (2010).
- [20] M. Merkl *et al.*, Phys. Rev. Lett. **104**, 073603 (2010).
- [21] J. Larson *et al.*, Phys. Rev. A **82**, 043620 (2010).
- [22] C. J. Pethick and H. Smith, *Bose-Einstein condensation*

*in dilute gases* (2nd ed. Cambridge Press, 2008).

- [23] S. Stringari, Phys. Rev. Lett. **77**, 2360 (1996).